MULTIGRID PRECONDITIONING FOR KRYLOV METHODS FOR TIME-HARMONIC MAXWELL'S EQUATIONS IN 3D

D.A. ARULIAH* AND U.M. ASCHER†

Abstract. We consider the rapid simulation of three-dimensional electromagnetic problems in geophysical parameter regimes where the conductivity may vary significantly and the range of frequencies is moderate. Toward developing a multigrid preconditioner, we present a Fourier analysis based on a finite-volume discretisation of a vector potential formulation of time-harmonic Maxwell's equations on a staggered grid in three dimensions. We prove grid-independent bounds on the eigenvalue and singular value ranges of the system obtained using a preconditioner based on exact inversion of the dominant diagonal blocks of the non-Hermitian coefficient matrix. This result implies that a preconditioner that uses single multigrid cycles to effect inversion of the diagonal blocks also yields a preconditioned system with ℓ_2-condition number bounded independent of the grid size.

We then present numerical examples for more realistic situations involving large variations in conductivity (i.e. jump discontinuities). Block-preconditioning with one multigrid cycle using J. Dendy's BOXMG solver is found to yield convergence in very few iterations, apparently independent of the grid size. The experiments show that the somewhat restrictive assumptions of the Fourier analysis do not prohibit it from describing the essential local behaviour of the preconditioned operator under consideration. A very efficient, practical solver is obtained.

Keywords: Multigrid preconditioning, Maxwell's equations, finite volume, Krylov methods, solution discontinuities.

1. Introduction. The need for calculating fast, accurate solutions of three-dimensional electromagnetic equations arises in many important application areas including, among others, geophysical surveys and medical imaging [6, 7, 20, 23, 28]. In remote sensing inverse problems, e.g. in geophysics, dozens, if not hundreds, of such systems are solved in the course of one data inversion. Consequently, there is much current interest in finding efficient numerical algorithms [5, 15, 19, 24].

Assuming a time-dependence $e^{-\imath\omega t}$ with frequency ω, Maxwell's equations in a three-dimensional domain Ω read

$$\nabla \times \boldsymbol{E} - \imath\omega\mu\boldsymbol{H} = \boldsymbol{0}, \tag{1.1a}$$

$$\nabla \times \boldsymbol{H} - (\sigma - \imath\omega\epsilon)\boldsymbol{E} = \boldsymbol{J^s}, \tag{1.1b}$$

where σ is the conductivity, ϵ the electrical permittivity, μ is the magnetic permeability and $\boldsymbol{J^s}$ is a known electric source current density. The physical properties $\epsilon > 0$, $\mu > 0$, and $\sigma \geq 0$ are known. The electric field $\boldsymbol{E}$ and the magnetic field $\boldsymbol{H}$ are unknown quantities. Throughout this paper, the permittivity is assumed spatially constant (i.e. $\epsilon \equiv \epsilon_0$) while the conductivity σ and the permeability μ are both spatially-varying, bounded and piecewise smooth. Further, the conductivity σ is slightly regularised by the substitution

$$\sigma \leftarrow \max(\sigma, \sigma_a), \tag{1.2}$$

with $\sigma_a > 0$ small (on the order of 10^{-9} to 10^{-6} S/m) to ensure $\sigma > 0$. The frequency range under consideration is restricted so that $\mu\epsilon_0\omega^2 L^2 \ll 1$, where L is a typical length scale [29]. Typical boundary conditions for (1.1) are described in [20].

*Fields Institute of Mathematical Sciences, Toronto, ON, M5T 3J1, Canada. (dhavide@fields.utoronto.ca). Supported in part under NSERC CRD Grant 80357.

†Department of Computer Science, University of British Columbia, Vancouver, BC, V6T 1Z4, Canada. (ascher@cs.ubc.ca). Supported in part under NSERC Research Grant 84306.

In previous work, we transformed the PDE system (1.1) to a weakly-coupled elliptic PDE system, derived a finite-volume discretisation on a staggered grid, and applied a preconditioned BiCGStab method (e.g., [4, 26]) to solve the resulting linear equations (see [3, 16, 17]). The corresponding stabilised PDE system considered is

$$\boldsymbol{\Delta}_\mu \boldsymbol{A} + \imath\omega(\sigma - \imath\omega\epsilon_0)\,(\boldsymbol{A} + \nabla\phi) = -\imath\omega \boldsymbol{J}^{\boldsymbol{s}}, \tag{1.3a}$$

$$\nabla \cdot \left((\sigma - \imath\omega\epsilon_0)\,(\boldsymbol{A} + \nabla\phi)\right) = -\nabla \cdot \boldsymbol{J}^{\boldsymbol{s}}, \tag{1.3b}$$

where the operator $\boldsymbol{\Delta}_\mu$ is defined by

$$\boldsymbol{\Delta}_\mu \boldsymbol{A} := \nabla\left(\mu^{-1}\nabla \cdot \boldsymbol{A}\right) - \nabla \times \left(\mu^{-1}\nabla \times \boldsymbol{A}\right). \tag{1.3c}$$

When μ is spatially homogeneous (i.e., constant), $\mu\boldsymbol{\Delta}_\mu$ simplifies to the ordinary vector Laplacian operator as in [3, 17]. The vector and scalar potential variables $\boldsymbol{A}$ and ϕ relate to the original variables $\boldsymbol{E}$ and $\boldsymbol{H}$ by substituting the Helmholtz decomposition [3, 14]

$$\boldsymbol{E} = \boldsymbol{A} + \nabla\phi, \tag{1.4a}$$

$$\nabla \cdot \boldsymbol{A} = 0, \tag{1.4b}$$

into (1.1). Boundary conditions and global constraints appropriate to close the PDE system (1.3) are

$$\boldsymbol{n} \times (\nabla \times \boldsymbol{A})|_{\partial\Omega} = \boldsymbol{0}, \tag{1.5a}$$

$$\boldsymbol{n} \cdot \boldsymbol{A}|_{\partial\Omega} = 0, \tag{1.5b}$$

$$\boldsymbol{n} \cdot [\sigma(\boldsymbol{A} + \nabla\phi)]|_{\partial\Omega} = -\boldsymbol{n} \cdot \boldsymbol{J}^{\boldsymbol{s}}|_{\partial\Omega}\,, \tag{1.5c}$$

$$\int_\Omega \phi \; dV = \int_\Omega (\mu^{-1}\nabla \cdot \boldsymbol{A}) \; dV \; = \; 0. \tag{1.5d}$$

The condition (1.5a) corresponds to $\boldsymbol{n} \times \boldsymbol{H}|_{\partial\Omega} = \boldsymbol{0}$ in the original variables [2, 16].

After discretising the system (1.3,1.5), applying Incomplete-LU (ILU, see [26, Chap. 10]) decomposition with a permissive threshold to the dominant diagonal blocks of the non-Hermitian coefficient matrix of the corresponding linear equations leads to a reliable preconditioner for Krylov-subspace methods [16, 17]. The possibility that just one multigrid cycle would be sufficiently powerful as a preconditioner to yield grid-independent convergence rates was noted earlier in other contexts by various researchers (see, e.g., [22] and references therein). Thus, our present goal is to develop a multigrid-preconditioning strategy for solving the problem (1.3,1.5).

We rescale the PDE (1.3) and review the discretisation in Section 2. In Section 3, we suggest a preconditioning strategy and present a Fourier analysis [8, 9, 13, 18, 25] to prove that using a preconditioner consisting of exact inverses of the dominant diagonal blocks yields a preconditioned linear system with eigenvalue and singular value ranges bounded independent of the grid spacing. This result in turn implies that using single multigrid W-cycles to approximate inversion of the diagonal blocks gives a preconditioned linear system with a grid-independent bound on the ℓ_2-condition number. Finally, in Section 4, we present results of numerical experiments using a multigrid-preconditioned solver. For the implementation of the preconditioner, we use Dendy's BOXMG code [11, 12]. Even in the general case of three-dimensional problems with variable coefficients and large discontinuities, the multigrid-preconditioned solver obtained is very efficient and practical.

2. Finite volume discretisation. It is convenient to introduce dimensionless quantities in (1.3) to simplify to presentation. If L, σ_0, and μ_0 are suitable scales of length, conductivity, and permeability respectively, we define the rescaled quantities

$$\begin{aligned} \overline{\boldsymbol{x}} &:= L^{-1}\boldsymbol{x}, \quad \overline{\sigma} := \sigma_0^{-1}(\sigma - \imath\omega\epsilon_0), \quad \overline{\mu} := \mu_0^{-1}\mu, \\ \overline{\phi} &:= L^{-1}\phi, \quad \overline{\boldsymbol{J^s}} := \sigma_0^{-1}\boldsymbol{J^s}, \end{aligned} \tag{2.1a}$$

and define the non-dimensional parameter

$$\chi := \omega\mu_0\sigma_0 L^2. \tag{2.1b}$$

In terms of the rescaled variables, the PDE (1.3) becomes

$$\overline{\boldsymbol{\Delta}}_{\overline{\mu}}\boldsymbol{A} + \imath\chi\overline{\sigma}\left(\boldsymbol{A} + \overline{\nabla\phi}\right) = -\imath\chi\overline{\boldsymbol{J^s}}, \tag{2.2a}$$

$$\overline{\nabla}\cdot\left(\overline{\sigma}\left(\boldsymbol{A} + \overline{\nabla\phi}\right)\right) = -\overline{\nabla}\cdot\overline{\boldsymbol{J^s}}, \tag{2.2b}$$

where bars above operators indicate differentiation with respect to the dimensionless position $\overline{\boldsymbol{x}}$ and the substitution of the dimensionless permeability $\overline{\mu}$ in the definition (1.3c). The fields $\boldsymbol{A}$, $\overline{\boldsymbol{J^s}}$ and $\overline{\phi}$ all have the same units; all the other quantities in (2.2) are dimensionless. Notice that the dimensionless conductivity $\overline{\sigma}$ is generally complex rather than real. In the sequel, we omit the bars except where explicitly necessary; when left out, all scale-related information lies in the dimensionless parameter χ.

To discretise the system (2.2), assume that Ω^h is the unit cube $[0,1]^3$ divided into a uniform $n \times n \times n$ union of non-overlapping cells of width $h := 1/n$ (this is a simplification of the grids considered in [3, 17]). The material properties σ and μ are assumed constant-valued within each cell. Further, assume that the current source $\boldsymbol{J^s}$ has no layers and that the normal components of $\boldsymbol{J^s}$ across cell interfaces are continuous.[1] Let $(A^x, A^y, A^z)^T$ denote the components of the vector potential field $\boldsymbol{A}$ in Cartesian coordinates. The discrete fields $\boldsymbol{A}^h$ and ϕ^h are defined on a staggered grid as illustrated in Figure 2.1. In particular, the discrete values ${A^x}_{i+\frac{1}{2},j,k}$, ${A^y}_{i,j+\frac{1}{2},k}$ and ${A^z}_{i,j,k+\frac{1}{2}}$ lie in the centres of corresponding cell faces and the discrete values $\phi_{i,j,k}$ lie at the centres of cells.

As in [3, 17], the non-Hermitian coefficient matrix for the discretised equations is

$$A := \begin{pmatrix} \boldsymbol{\Delta}_\mu^h + \imath\chi\sigma^h & \imath\chi\sigma^h(\nabla)^h \\ (\nabla\cdot)^h\sigma^h & (\nabla\cdot)^h\sigma^h(\nabla)^h \end{pmatrix}. \tag{2.3}$$

In (2.3), the blocks are discretisations of various operators on a staggered grid subject to the boundary conditions (1.5) with lexicographic ordering. The operator ∇^h is the discretisation of the gradient operator; $(\nabla\cdot)^h$ is the discretisation of the divergence operator; σ^h is the staggered grid discretisation of the operator σI (using harmonic averages of values of σ in adjacent cells, e.g., [27]); and $\boldsymbol{\Delta}_\mu^h$ is the discretisation of the operator $\boldsymbol{\Delta}_\mu$ as in (1.3c). Within $\boldsymbol{\Delta}_\mu^h$ in (2.3), there are two distinct discretisations of the curl operator and the permeability operator μ respectively to account for the different spaces in which the discrete vector and scalar grid functions lie; for details, see [2, 16]. Notice that $\boldsymbol{\Delta}_\mu^h$ and σ^h are in turn 3×3 block matrices that act on the space of discrete vector fields with components normal to cell faces. Further, $(\nabla)^h$

[1] In practice, the grid is chosen such that source singularities, if they occur, are contained inside grid cells.

FIG. 2.1. *Staggered grid discretisation. The discrete vector field* $\boldsymbol{A}^h$ *at centres of cell faces and the discrete scalar field* ϕ^h *at centres of cells.*

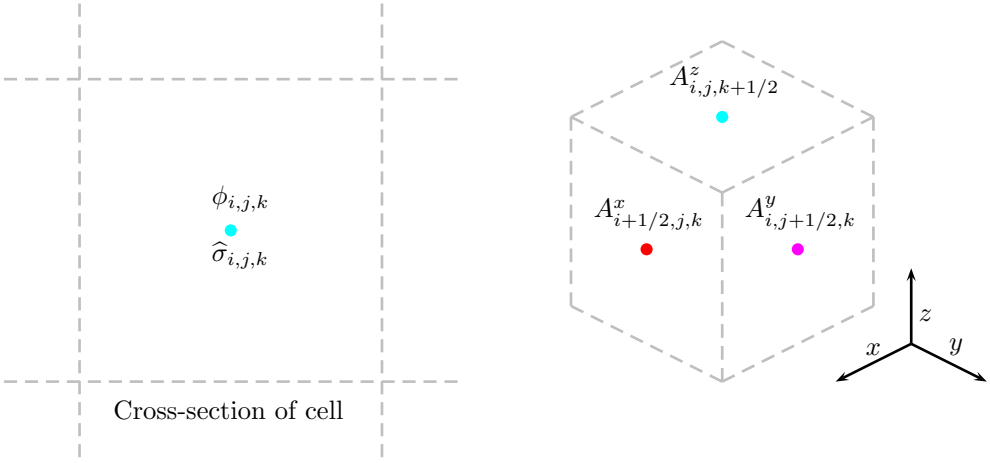

is a 3×1 block matrix (mapping discrete scalar fields to discrete vector fields) and $(\nabla\cdot)^h$ is a 1×3 block matrix (mapping discrete vector fields to discrete scalar fields).

Under the assumption of constant permeability, the dimensionless $\overline{\mu} \equiv 1$ and so $\boldsymbol{\Delta}^h_\mu$ reduces to a standard 7-point discretisation of the vector Laplacian operator. In this case, considering (2.3) as a 4×4 block matrix, the operators in the first block row of A are

$$\begin{aligned}\left[\Delta^h A^{x\,h}\right]_{i+\frac{1}{2},j,k} + \imath\chi\sigma_{i+\frac{1}{2},j,k} = \frac{1}{h^2}\Big(&A^x{}_{i+\frac{3}{2},j,k} + A^x{}_{i+\frac{1}{2},j+1,k} + A^x{}_{i+\frac{1}{2},j,k+1} \\ &+ A^x{}_{i-\frac{1}{2},j,k} + A^x{}_{i+\frac{1}{2},j-1,k} + A^x{}_{i+\frac{1}{2},j,k-1} \\ &+ (-6 + \imath\chi h^2\sigma_{i+\frac{1}{2},j,k})A^x{}_{i+\frac{1}{2},j,k}\Big), \qquad (2.4a)\end{aligned}$$

$$\left[(\sigma^h(\nabla)^h)^x\phi^h\right]_{i+\frac{1}{2},j,k} = \frac{1}{h}\sigma_{i+\frac{1}{2},j,k}\left(\phi_{i+1,j,k} - \phi_{i,j,k}\right). \qquad (2.4b)$$

For the more general variable-μ case, see [2, 17] for details. The second and third block rows are defined analogously. The last block row details equations that are centered at cell centres and defined by

$$\begin{aligned}\left[(\nabla\cdot)^h\sigma^h\boldsymbol{A}^h\right]_{i,j,k} = \frac{1}{h}\Big(&\sigma_{i+\frac{1}{2},j,k}A^x{}_{i+\frac{1}{2},j,k} - \sigma_{i-\frac{1}{2},j,k}A^x{}_{i-\frac{1}{2},j,k} \\ &+ \sigma_{i,j+\frac{1}{2},k}A^y{}_{i,j+\frac{1}{2},k} - \sigma_{i,j-\frac{1}{2},k}A^y{}_{i,j-\frac{1}{2},k} \\ &+ \sigma_{i,j,k+\frac{1}{2}}A^z{}_{i,j,k+\frac{1}{2}} - \sigma_{i,j,k-\frac{1}{2}}A^z{}_{i,j,k-\frac{1}{2}}\Big), \qquad (2.5a)\end{aligned}$$

$$\begin{aligned}\left[(\nabla\cdot)^h\sigma^h(\nabla)^h\phi^h\right]_{i,j,k} = \frac{1}{h^2}\Big(&\sigma_{i+\frac{1}{2},j,k}\phi_{i+1,j,k} + \sigma_{i,j+\frac{1}{2},k}\phi_{i,j+1,k} + \sigma_{i,j,k+\frac{1}{2}}\phi_{i,j,k+1} \\ &+ \sigma_{i-\frac{1}{2},j,k}\phi_{i-1,j,k} + \sigma_{i,j-\frac{1}{2},k}\phi_{i,j-1,k} + \sigma_{i,j,k-\frac{1}{2}}\phi_{i,j,k-1} \\ &- \Big(\sigma_{i+\frac{1}{2},j,k} + \sigma_{i,j+\frac{1}{2},k} + \sigma_{i,j,k+\frac{1}{2}} \\ &\quad + \sigma_{i-\frac{1}{2},j,k} + \sigma_{i,j-\frac{1}{2},k} + \sigma_{i,j,k-\frac{1}{2}}\Big)\phi_{i,j,k}\Big). \qquad (2.5b)\end{aligned}$$

3. Fourier Analysis. Given the coefficient matrix A as in (2.3), we wish to find suitable preconditioners for solving associated linear systems. The matrix A decomposes naturally as

$$A = A_1 + \imath\chi A_2 \tag{3.1a}$$

where

$$A_1 := \begin{pmatrix} \boldsymbol{\Delta}_{\mu}^{h} & \\ (\nabla\cdot)^h\sigma^h & (\nabla\cdot)^h\sigma^h(\nabla)^h \end{pmatrix} \text{ and} \tag{3.1b}$$

$$A_2 := \begin{pmatrix} \sigma^h & \sigma^h(\nabla)^h \\ & \end{pmatrix}. \tag{3.1c}$$

The matrices A_1 and A_2 are generally complex unless the term $\imath\omega\epsilon_0$ is ignored in $\overline{\sigma}$ (the quasi-static assumption [29]). For h sufficiently small, the diagonal blocks of A_1 dominate all other blocks; hence, a logical choice of preconditioners is the block-diagonal matrix M given by

$$M := \begin{pmatrix} \boldsymbol{\Delta}_{\mu}^{h} & \\ & (\nabla\cdot)^h\sigma^h(\nabla)^h \end{pmatrix}. \tag{3.2}$$

Indeed, the matrix M is an optimal preconditioner for the matrix A_1 in that all the eigenvalues of $M^{-1}A_1$ are one and its minimal polynomial is of degree two. Thus, it follows that using M as a preconditioner for A will also be useful provided that χ is sufficiently small.

To get a more quantitative understanding of the efficacy of M as a preconditioner for A, we now consider the system (2.2) and its discretisation (2.3) under simplifying assumptions that ensure that the eigenvectors of all the blocks of A in (2.3) are Fourier modes [8, 9]. In particular, for discrete wavenumbers $0 \le \alpha, \beta, \gamma \le n-1$, we want the grid function $\psi^{\alpha\beta\gamma}$ given by

$$\psi_{ijk}^{\alpha\beta\gamma} := e^{(2\pi\alpha ih)\imath} e^{(2\pi\beta jh)\imath} e^{(2\pi\gamma kh)\imath} \qquad (i,j,k = 0,1,\ldots n-1) \tag{3.3}$$

to be an eigenvector of all the blocks of A in (2.3). This is true under the assumptions that

1. the grid is uniform;
2. the boundary conditions are periodic[2]; and
3. the dimensionless coefficients are constant, i.e., $\overline{\sigma} \equiv 1$ and $\overline{\mu} \equiv 1$.

Under the second assumption, upon discretisation, the indexing in (2.4) and (2.5) is done in arithmetic modulo n. For instance, grid points on, say, the top boundary are identified with opposite points on the bottom boundary, and centers of cells touching the top boundary are considered as neighbours of centers of cells opposite touching the bottom boundary. The scalar grid functions $A^{x\,h}$, $A^{y\,h}$, $A^{z\,h}$, and ϕ^h each consist of $N := n^3$ unknowns, the matrix blocks in (2.3) are square of dimension $N \times N$, and the resulting system to be solved has dimension $4N \times 4N$.

[2]For a class of realistic geophysical problems, the fields are expected to vanish or decay in the absence of source currents, and the sources are frequently of compact support. Thus, for a sufficiently large domain Ω, the effect of boundary data on the fields inside the domain is often negligible. In such cases, the assumption of periodicity in the analysis is particularly reasonable and does not compromise the model.

The quasi-static assumption is implicit in the third assumption, i.e., the term $\imath\omega\epsilon_0$ is dropped in the definition $\overline{\sigma}$ in (2.1a). This simplifies the presentation without loss of essence in the obtained theoretical results. Thus, with the third assumption above, the block matrix σ^h is replaced by I_{3N} and $\mathbf{\Delta}_\mu^h$ is replaced by $\mathbf{\Delta}^h$ in (2.3). In the experiments reported in Section 4, we drop most of the restrictive assumptions of the analysis of the present section.

Thus, with these assumptions, the coefficient matrix in (2.3) is

$$A = \begin{pmatrix} \Delta^h + \imath\chi I_N & & & \imath\chi D_x^h \\ & \Delta^h + \imath\chi I_N & & \imath\chi D_y^h \\ & & \Delta^h + \imath\chi I_N & \imath\chi D_z^h \\ -(D_x^h)^* & -(D_y^h)^* & -(D_z^h)^* & \Delta^h \end{pmatrix} \tag{3.4}$$

In (3.4), the matrices D_x^h, D_y^h, and D_z^h correspond to discretisations of first-order derivative operators with periodic boundary conditions. Assuming standard lexicographic ordering for the unknowns describing the grid functions,

$$\begin{aligned} D_x^h &:= I_n \otimes I_n \otimes D^- \in \mathbb{C}^{N\times N}, \\ D_y^h &:= I_n \otimes D^- \otimes I_n \in \mathbb{C}^{N\times N}, \text{ and} \\ D_z^h &:= D^- \otimes I_n \otimes I_n \in \mathbb{C}^{N\times N}. \end{aligned}$$

Here,

$$D^- := \frac{1}{h}\begin{pmatrix} 1 & & & -1 \\ -1 & 1 & & \\ & \ddots & \ddots & \\ & & -1 & 1 \end{pmatrix} \in \mathbb{C}^{n\times n} \tag{3.5}$$

is the matrix for the periodic primitive backward difference operator in one dimension, and $\otimes$ denotes the conventional Kronecker product (e.g. [10, p. 274]). Likewise, the matrices $-(D_x^h)^*$, $-(D_y^h)^*$, and $-(D_z^h)^*$ in the fourth block row of (3.4) correspond to forward difference operators. Finally, the discretisation Δ^h of the Laplacian operator Δ with periodic boundary conditions satisfies

$$\Delta^h = -D_x^h(D_x^h)^* - D_y^h(D_y^h)^* - D_z^h(D_z^h)^*.$$

The eigenvalues of the difference operators in (3.4) are

$$d_x{}^{\alpha\beta\gamma} := h^{-1}\left(1 - e^{-(2\alpha\pi h)\imath}\right) \text{ for } D_x^h, \tag{3.6a}$$

$$d_y{}^{\alpha\beta\gamma} := h^{-1}\left(1 - e^{-(2\beta\pi h)\imath}\right) \text{ for } D_y^h, \tag{3.6b}$$

$$d_z{}^{\alpha\beta\gamma} := h^{-1}\left(1 - e^{-(2\gamma\pi h)\imath}\right) \text{ for } D_z^h, \text{ and} \tag{3.6c}$$

$$\delta^{\alpha\beta\gamma} := -\frac{4}{h^2}\left(\sin^2(\alpha\pi h) + \sin^2(\beta\pi h) + \sin^2(\gamma\pi h)\right) \text{ for } \Delta^h, \tag{3.6d}$$

with common eigenvector $\psi^{\alpha\beta\gamma}$ as in (3.3) ($\alpha,\beta,\gamma = 0,\ldots,n-1$). In particular, the nonzero eigenvalues $\delta^{\alpha\beta\gamma}$ of Δ^h satisfy

$$\begin{aligned} &0 < \frac{h^2}{12} \le -\frac{1}{\delta^{\alpha\beta\gamma}} \le \frac{h^2}{4\sin^2(\pi h)} \le \frac{1}{16} \\ &(\alpha,\beta,\gamma = 0,\ldots,n-1; \alpha^2+\beta^2+\gamma^2 > 0) \end{aligned} \tag{3.7}$$

for $n \geq 2$. The upper bound of $1/16$ on $-1/\delta^{\alpha\beta\gamma}$ is obtained for a very coarse mesh when $n = 2$; as n increases, the actual maximum decreases.

Knowing the eigenvalues (3.6) of the blocks of A in (3.4), we want to determine the eigenvalues and singular values of the preconditioned iteration matrix $M^{-1}A$, where M from (3.2) now has the form

$$M = \operatorname{diag}(\Delta^h, \Delta^h, \Delta^h, \Delta^h). \tag{3.8}$$

Under the assumptions of the current section, the matrix M is real and consists of the dominant diagonal blocks of the matrix A_1 in (3.1).

Note that the solution u of $\Delta u = b$ with periodic boundary conditions is determined only up to a constant. Thus, M in (3.8) has a zero eigenvalue of multiplicity four (the corresponding eigenvectors are columns of $I_4 \otimes \psi^{000}$). Likewise, A has a zero eigenvalue of multiplicity one. However, as in [13], if S_0 denotes the space spanned by the constant grid function $\psi^{000} \in \mathbb{C}^N$ and $S_0^\perp$ denotes the orthogonal complement of S_0 in $\mathbb{C}^N$, then $\Delta^h|_{S_0^\perp}$ is invertible. Further, the operator $(\Delta^h|_{S_0^\perp})^{-1}$ extends to an operator $(\Delta^h)_*^{-1}$ defined over all of $\mathbb{C}^N$ by defining it to be 0 on S_0. Thus, it makes sense to consider eigenvalue ranges for M and A which exclude the zero eigenvalues. This is achieved by imposing the condition

$$\alpha^2 + \beta^2 + \gamma^2 > 0,$$

as in (3.7). Under this condition, with a slight abuse of notation, we subsequently refer to A and M as being nonsingular.

Having established that the blocks of A in (3.4) all share common eigenvectors and that considering the operator $M^{-1}A$ makes sense, we wish to derive bounds on the eigenvalue range and the ℓ_2-condition number of $M^{-1}A$. To explicitly determine and bound $\kappa_2(M^{-1}A)$, we determine the singular values of $M^{-1}A$ since

$$\kappa_2(M^{-1}A) = \frac{\eta_{\max}}{\eta_{\min}},$$

where $\eta_{\max}$ and $\eta_{\min}$ are the largest and smallest singular values of $M^{-1}A$ respectively. The eigenvalues and singular values of this matrix can be determined by considering the eigenvalues of a 4×4 matrix with the same structure, as Lemma 3.1 indicates.

LEMMA 3.1. *Let $C \in \mathbb{C}^{(mn)\times(mn)}$ be a block matrix with blocks $C_{ij} \in \mathbb{C}^{n\times n}$ $(i, j = 1, \ldots, m)$. Let the blocks C_{ij} all share a common eigenvector $\boldsymbol{v} \in \mathbb{C}^n$ with corresponding eigenvalues $\gamma_{ij} \in \mathbb{C}$ $(i, j = 1, \ldots, m)$. Furthermore, let $G = (\gamma_{ij}) \in \mathbb{C}^{m\times m}$ have the eigenvalues γ_{ij} as its elements, and let λ be an eigenvalue of G with an eigenvector $\boldsymbol{u} \in \mathbb{C}^m$. Then λ is also an eigenvalue of C with an eigenvector $\boldsymbol{u} \otimes \boldsymbol{v}$.*

For a proof of this lemma, see [2] or [31, p.136].

Next, we find the eigenvalues and singular values of the 4×4 matrix corresponding to $M^{-1}A$ in Fourier space. Recall the notation (2.1b).

LEMMA 3.2. *Let $dx, dy, dz \in \mathbb{C}$ be prescribed scalars such that $\delta := -dxdx^* - dydy^* - dzdz^* < 0$. Given $\sigma, \chi > 0$, define the complex 4×4 matrix $\widetilde{M}^{-1}\widetilde{A}$, where*

$$\widetilde{M} := \begin{pmatrix} \delta & & & \\ & \delta & & \\ & & \delta & \\ & & & \delta \end{pmatrix} \quad \text{and} \quad \widetilde{A} := \begin{pmatrix} \delta + \imath\chi & & & \imath\chi dx \\ & \delta + \imath\chi & & \imath\chi dy \\ & & \delta + \imath\chi & \imath\chi dz \\ -dx^* & -dy^* & -dz^* & \delta \end{pmatrix}.$$

Then, the eigenvalues $\widetilde{\lambda}$ *of* $\widetilde{M}^{-1}\widetilde{A}$ *are*

$$\widetilde{\lambda}_1 := 1 + \frac{\imath}{2\delta}\left(\chi + \sqrt{\chi(\chi - 4\delta\imath)}\right), \tag{3.9a}$$

$$\widetilde{\lambda}_2 = \widetilde{\lambda}_3 := 1 + \frac{\chi}{\delta}\imath, \tag{3.9b}$$

$$\widetilde{\lambda}_4 := 1 + \frac{\imath}{2\delta}\left(\chi - \sqrt{\chi(\chi - 4\delta\imath)}\right). \tag{3.9c}$$

Further, the singular values $\widetilde{\eta}$ *of* $\widetilde{M}^{-1}\widetilde{A}$ *are*

$$\widetilde{\eta}_1 := \left[1 + \frac{c}{2} + \frac{1}{2}\sqrt{c(c+4)}\right]^{\frac{1}{2}}, \tag{3.10a}$$

$$\widetilde{\eta}_2 = \widetilde{\eta}_3 := \left[1 + \frac{\chi^2}{\delta^2}\right]^{\frac{1}{2}}, \tag{3.10b}$$

$$\widetilde{\eta}_4 := \left[1 + \frac{c}{2} - \frac{1}{2}\sqrt{c(c+4)}\right]^{\frac{1}{2}}, \tag{3.10c}$$

where $c = c(-\frac{1}{\delta}, \chi) := \left(-\frac{1}{\delta}\right)\left(1 + \chi^2\left(1 - \frac{1}{\delta}\right)\right) > 0$.

Proof. Although the derivation of (3.9) and (3.10) requires tedious algebraic manipulations, the formulae are verifiable directly by inspection. □

Note that the eigenvalues and singular values of $\widetilde{M}^{-1}\widetilde{A}$ in Lemma 3.2 depend only on the parameters $\delta < 0$ and $\chi > 0$. We next derive bounds for the moduli of the eigenvalues $|\widetilde{\lambda}|$ in (3.9) and the singular values $\widetilde{\eta}$ in (3.10), hence bounding their respective ranges.

LEMMA 3.3. *Assume* $0 < -1/\delta < \frac{1}{16}$. *Then, the eigenvalues* $\widetilde{\lambda}$ *of* $\widetilde{M}^{-1}\widetilde{A}$ *given in* (3.9) *all satisfy*

$$0 < \widetilde{\lambda}_{\min} \le \left|\widetilde{\lambda}\right| \le \widetilde{\lambda}_{\max}$$

and the singular values $\widetilde{\eta}$ *given in* (3.10) *all satisfy*

$$0 < \widetilde{\eta}_{\min} \le \widetilde{\eta} \le \widetilde{\eta}_{\max},$$

where $\widetilde{\lambda}_{\min}$, $\widetilde{\lambda}_{\max}$, $\widetilde{\eta}_{\min}$, *and* $\widetilde{\eta}_{\max}$ *are positive constants that depend on* χ *but not on* δ. *Further,*

$$\frac{\widetilde{\lambda}_{\max}}{\widetilde{\lambda}_{\min}} = O(\chi^2) \text{ and } \kappa_2(\widetilde{M}^{-1}\widetilde{A}) = \frac{\widetilde{\eta}_{\max}}{\widetilde{\eta}_{\min}} = O(\chi^2).$$

Proof. Denote $\zeta = \sqrt{\chi^2 + 16\delta^2} > \chi$. From (3.9), we find

$$\left|\widetilde{\lambda}_1\right| = \left[\frac{\chi}{4\delta^2}\left(\chi + \zeta + \sqrt{2\chi}\sqrt{\zeta + \chi}\right) - \frac{\sqrt{2\chi}}{2\delta}\sqrt{\zeta - \chi} + 1\right]^{\frac{1}{2}}, \tag{3.11a}$$

$$\left|\widetilde{\lambda}_2\right| = \left|\widetilde{\lambda}_3\right| = \left[1 + \frac{\chi^2}{\delta^2}\right]^{\frac{1}{2}}, \tag{3.11b}$$

$$\left|\widetilde{\lambda}_4\right| = \left[\frac{\chi}{4\delta^2}\left(\chi + \zeta - \sqrt{2\chi}\sqrt{\zeta + \chi}\right) + \frac{\sqrt{2\chi}}{2\delta}\sqrt{\zeta - \chi} + 1\right]^{\frac{1}{2}}. \tag{3.11c}$$

It follows from the analytic expressions in (3.11) that

$$|\widetilde{\lambda}_1| \geq |\widetilde{\lambda}_2| = |\widetilde{\lambda}_3| \geq |\widetilde{\lambda}_4|$$

for any valid choices of χ and δ. Examining $|\widetilde{\lambda}_1|$ and $|\widetilde{\lambda}_4|$ as δ varies over the interval $(-\infty, -16)$, we find

$$\widetilde{\lambda}_{\max} := \max\left\{\left|\widetilde{\lambda}_1\right| : \delta \in (-\infty, -16)\right\} = \left|\widetilde{\lambda}_1\right|_{\delta=-16}, \text{ and}$$
$$\widetilde{\lambda}_{\min} := \min\left\{\left|\widetilde{\lambda}_4\right| : \delta \in (-\infty, -16)\right\} = \left|\widetilde{\lambda}_4\right|_{\delta=-16}.$$

Thus,

$$\frac{\widetilde{\lambda}_{\max}}{\widetilde{\lambda}_{\min}} = \left|\frac{\widetilde{\lambda}_1}{\widetilde{\lambda}_4}\right|_{\delta=-16} = \frac{\chi^2}{256} + O(1) = O(\chi^2).$$

Examining the singular values (3.10) in the same manner, we find

$$\widetilde{\eta}_1 \geq \widetilde{\eta}_2 = \widetilde{\eta}_3 \geq \widetilde{\eta}_4.$$

Thus,

$$\widetilde{\eta}_{\max} := \max\{\widetilde{\eta}_1 : \delta \in (-\infty, -16)\} = \eta_1|_{\delta=-16}, \text{ and}$$
$$\widetilde{\eta}_{\min} := \min\{\widetilde{\eta}_4 : \delta \in (-\infty, -16)\} = \eta_4|_{\delta=-16}.$$

Hence,

$$\frac{\widetilde{\eta}_{\max}}{\widetilde{\eta}_{\min}} = \frac{17}{256}\chi^2 + O(1) = O(\chi^2).$$

□

The preceding lemmata give us the desired eigenvalues and singular values of the underlying matrix $M^{-1}A$ for the preconditioned system. Combining these results, we obtain Theorem 3.4.

THEOREM 3.4. *For $\alpha, \beta, \gamma = 0, 1, \ldots, n-1$ and $\alpha^2 + \beta^2 + \gamma^2 > 0$, the nonzero eigenvalues and the singular values of $M^{-1}A$ are given by*

$$\lambda_1^{\alpha\beta\gamma} = 1 + \frac{\imath}{2\delta^{\alpha\beta\gamma}}\left(\chi + \sqrt{\chi(\chi - 4\delta^{\alpha\beta\gamma}\imath)}\right), \tag{3.12a}$$
$$\lambda_2^{\alpha\beta\gamma} = \lambda_3^{\alpha\beta\gamma} := 1 + \frac{\chi}{\delta^{\alpha\beta\gamma}}\imath, \tag{3.12b}$$
$$\lambda_4^{\alpha\beta\gamma} = 1 + \frac{\imath}{2\delta^{\alpha\beta\gamma}}\left(\chi - \sqrt{\chi(\chi - 4\delta^{\alpha\beta\gamma}\imath)}\right), \tag{3.12c}$$

and

$$\eta_1^{\alpha\beta\gamma} := \left[1 + \frac{c^{\alpha\beta\gamma}}{2} + \frac{1}{2}\sqrt{c^{\alpha\beta\gamma}(c^{\alpha\beta\gamma} + 4)}\right]^{\frac{1}{2}}, \tag{3.13a}$$
$$\eta_2^{\alpha\beta\gamma} = \eta_3^{\alpha\beta\gamma} := \left[1 + \frac{\chi^2}{\delta^{\alpha\beta\gamma 2}}\right]^{\frac{1}{2}}, \tag{3.13b}$$
$$\eta_4^{\alpha\beta\gamma} := \left[1 + \frac{c^{\alpha\beta\gamma}}{2} - \frac{1}{2}\sqrt{c^{\alpha\beta\gamma}(c^{\alpha\beta\gamma} + 4)}\right]^{\frac{1}{2}} \tag{3.13c}$$

respectively, where $c^{\alpha\beta\gamma} = c(-\frac{1}{\delta^{\alpha\beta\gamma}}, \chi) := \left(-\frac{1}{\delta^{\alpha\beta\gamma}}\right)\left(1 + \chi^2\left(1 - \frac{1}{\delta^{\alpha\beta\gamma}}\right)\right) > 0$. *Furthermore, for* $n > 2$, *the nonzero eigenvalues and singular values of* $M^{-1}A$ *are bounded above and below independent of the grid size* h. *Defining*

$$\lambda_{\min} = \min\{|\lambda_i| : 1 \le i \le 4\}, \qquad \lambda_{\max} = \max\{|\lambda_i| : 1 \le i \le 4\},$$
$$\eta_{\min} = \min\{\eta_i : 1 \le i \le 4\}, \qquad \eta_{\max} = \max\{\eta_i : 1 \le i \le 4\},$$

the eigenvalue range $\lambda_{\max}/\lambda_{\min}$ *and the* ℓ_2*-condition number* $\kappa_2(M^{-1}A) = \eta_{\max}/\eta_{\min}$ *are bounded independent of the grid, but increase quadratically with the parameter* $\chi := \omega\mu_0\sigma_0 L^2$:

$$\frac{\lambda_{\max}}{\lambda_{\min}} \le \frac{\widetilde{\lambda}_{\max}}{\widetilde{\lambda}_{\min}} = O(\chi^2) \text{ and } \kappa_2(M^{-1}A) = \frac{\eta_{\max}}{\eta_{\min}} \le \frac{\widetilde{\eta}_{\max}}{\widetilde{\eta}_{\min}} = O(\chi^2).$$

Proof. The eigenvalues (3.12) and singular values (3.13) of $M^{-1}A$ are derived directly from the eigenvalues (3.9) and singular values (3.10) of $\widetilde{M}^{-1}\widetilde{A}$ in Lemma 3.2 by applying Lemma 3.1. Then, the bounds $\widetilde{\lambda}_{\max}/\widetilde{\lambda}_{\min}$ and $\widetilde{\eta}_{\max}/\widetilde{\eta}_{\min}$ follow from Lemma 3.3. □

In Figure 3.1, we plot the curves based on the above estimates for the eigenvalue range and the ℓ_2-condition number of $\widetilde{M}^{-1}\widetilde{A}$ as a function of χ (which are in fact the bounds $\widetilde{\lambda}_{\max}/\widetilde{\lambda}_{\min}$ and $\widetilde{\eta}_{\max}/\widetilde{\eta}_{\min}$ from Lemma 3.3). We also plot the actual values of $\lambda_{\max}/\lambda_{\min}$ and $\eta_{\max}/\eta_{\min}$ as computed from Theorem 3.4 in the case $n = 10^4$.

FIG. 3.1. *Eigenvalue range* $\widetilde{\lambda}_{\max}/\widetilde{\lambda}_{\min}$ *and the* ℓ_2*-condition number* $\widetilde{\eta}_{\max}/\widetilde{\eta}_{\min}$ *as a function of* χ *based on the formulae in Lemma 3.3. Also plotted are actual values* ($\lambda_{\max}/\lambda_{\min}$ *and* $\eta_{\max}/\eta_{\min}$, *respectively) for* $n = 10^4$.

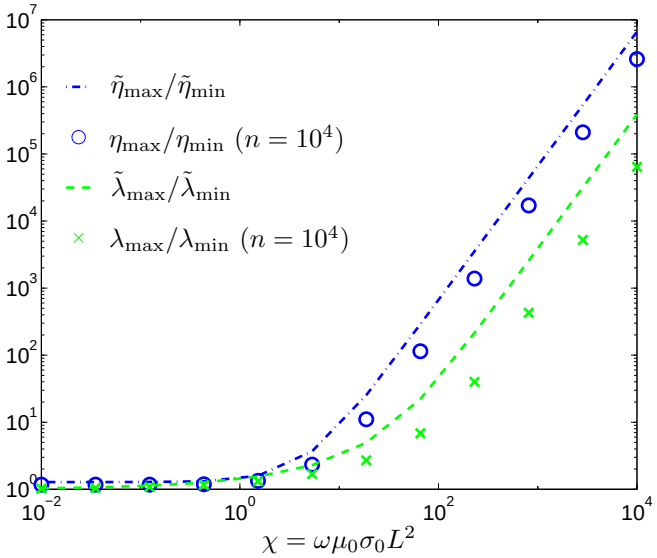

Notice that Lemma 3.3 also indicates that the ratio of the largest to smallest eigenvalues significantly underestimates the ratio of the largest to smallest singular values (which is the ℓ_2-condition number) in the case that χ is large. This is also reflected in a lower degree of diagonal dominance in A and $M^{-1}A$ (for a fixed mesh size h) as ω increases.

The practical implication of Theorem 3.4 is that the number of iterations required for convergence (up to a set positive tolerance) of a Krylov method for (3.4) preconditioned by exact inversions of the real parts of the leading blocks is expected to be small and independent of the grid size. As the frequency ω increases in a range where $\omega\mu_0\sigma_0 L^2 \gg 1$, the number of iterations required for convergence may be expected to increase like ω^2.

The full inversions of the main diagonal blocks of M are prohibitively expensive for a preconditioner. Instead, we now consider applying just one multigrid cycle. Denote by B the approximate inverse for M obtained in this way. It is well-known (e.g., [18, 30]) that for a W-cycle using standard grid transfer and coarse grid operators and a sufficiently good smoothing rate (which may be achieved, e.g., by two (point) red-black Gauss-Seidel sweeps before and after the coarse grid correction), there is a constant c independent of the grid size such that

$$\|I - BM\| \leq c < 1.$$

This implies that the ℓ_2-condition number of BM is bounded. Writing

$$\kappa_2(BA) \leq \kappa_2(BM)\ \kappa_2(M^{-1}A)$$

and applying Theorem 3.4 now yields a similar result for the one-multigrid-cycle preconditioner.

COROLLARY 3.5. *The ℓ_2-condition number of BA, where B is the preconditioning matrix effecting one multigrid W-cycle, is bounded independent of the grid size h. The bound on the condition number increases quadratically with the parameter $\chi = \omega\mu_0\sigma_0 L^2$.*

4. Numerical Experiments. In the following experiments, the permeability $\epsilon = \epsilon_0 = 8.8542 \times 10^{-12}$ F/m and the permittivity $\mu = \mu_0 = 4\pi \times 10^{-7}$ H/m are fixed constants. The domain Ω is the cube $[-1,1]^3$ and the length scale $L =$ 1m. The homogeneous boundary conditions (1.5) are imposed on $\partial\Omega$ as described in Section 2; although the use of the boundary conditions (1.5) requires a domain Ω that is sufficiently large, the experiments here focus on the performance of iterative solvers based on multigrid algorithms; this is unrelated to the specific boundary conditions implemented [8].

As in [3, 16, 17], the grids used are either uniform or exponentially-widening, and preconditioned BiCGStab [4] is used to solve the linear systems generated by the discretisation. As a convergence criterion for all BiCGStab iterations, we require a reduction of the relative residual to within a tolerance of 10^{-7}. Results from all experiments are given in terms of iteration counts.

We contrast the performances of several preconditioning strategies.

1. Exact solves of diagonal blocks (M_E): The real parts of the diagonal blocks, namely

$$\operatorname{diag}\left(\Delta^h + \omega^2\epsilon I, \Delta^h + \omega^2\epsilon I, \Delta^h + \omega^2\epsilon I, (\nabla\cdot)^h\sigma^h(\nabla)^h\right),$$

   are inverted exactly (by iterating a multigrid solver to convergence) in each iteration. For the magnitudes of $\omega^2\epsilon$ considered, the difference between this preconditioning strategy and the one analyzed in Section 3 is negligible.
2. Multigrid preconditioning (M_M): Single V(2,1)-cycles [8, 18] are applied for each of the diagonal blocks to approximate the effect of M_E. For the (1,1), (2,2), and (3,3) blocks, we use point red-black Gauss-Seidel smoothing if the

grid is uniform, and alternating-plane smoothing otherwise. For the (4,4) block, we use alternating-plane smoothing regardless of the grid.

3. ILU preconditioning (M_I): An incomplete-LU factorisation is computed (see [4, 26]) using the real part of the diagonal blocks of the coefficient matrix A. We use 10^{-2} for the drop tolerance.
4. SSOR preconditioning (M_S): We use the value 1.0 for the over-relaxation parameter [4].

The multigrid solver used is Dendy's code BOXMG (a black-box multigrid solver, see [11, 12]). For Poisson or simple Helmholtz problems on uniform grids, point red-black Gauss-Seidel smoothing cheaply inverts the $(1,1)$, $(2,2)$, and $(3,3)$ blocks. For the inhomogeneous diffusion operator in the (4,4) block and for problems on non-uniform grids, alternating-plane smoothing is required to achieve reasonable multigrid performance, as observed in [1, 11, 12]. This gives a slight cause for concern, since the implementation of alternating-plane smoothing is quite costly; however, for large, highly inhomogeneous problems, the multigrid preconditioner applied with alternating-plane smoothing yields a robust solver.

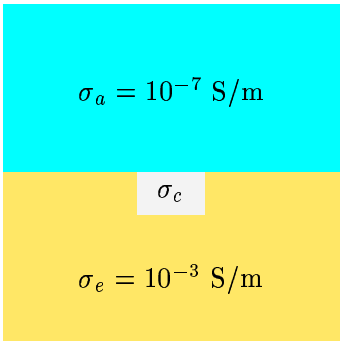

FIG. 4.1. *Cross-section of a conducting block in a half-space*

For the conductivity σ in Ω, we choose

$$\sigma(x,y,z) = \begin{cases} \sigma_a, & z > 0; \\ \sigma_c, & |x| \le \frac{1}{5}, |y| \le \frac{1}{5}, -\frac{1}{5} \le z \le 0; \\ \sigma_e, & \text{otherwise}, \end{cases}$$

for the experiments. This models a conducting block of conductivity σ_c embedded in a half-space (i.e. at the interface between ground and air). The conductivity σ_e of the earth is $\sigma_e = 10^{-3}$ S/m and the conductivity σ_a of the air is $\sigma_a = 10^{-7}$ S/m (which regularises σ as in (1.2)).

Thus, in our experiments, we vary the parameters σ_c and ω to compare performances of various preconditioners. We also vary the source term $\boldsymbol{J^s}$ in (1.3). The applied electromagnetic sources are electric dipoles or magnetic current loops as in [16, 29][3]

Consider first varying ω over the moderate range $[10^0, 10^4]$ Hz, and varying σ_c over the range $[10^{-2}, 10^2]$ S/m. These ranges translate to the parameter χ in (2.1b) lying

[3]Using traditional discretisations of Maxwell's equations (1.1), convergence rates for Krylov-subspace iterations tend to be far worse for experiments with electric sources than with magnetic sources (see [16, 21]).

in the interval $[4\pi \times 10^{-9}, 4\pi \times 10^{-1}]$. The jump discontinuities in σ for this range of σ_c are between 5 and 9 orders of magnitude. For an electric dipole source, the results when discretised on uniform and non-uniform grids are tabulated in Tables 4.1 and 4.2 respectively. Tables 4.3 and 4.4 present results from similar trials on uniform and non-uniform grids respectively with a magnetic (divergence-free) source term instead.

Uniform grids													
σ_c	# of	$\omega = 10^0$Hz				$\omega = 10^2$Hz				$\omega = 10^4$Hz			
(S/m)	cells	M_E	M_M	M_I	M_S	M_E	M_M	M_I	M_S	M_E	M_M	M_I	M_S
10^{-2}	10^3	1	3	7	19	3	3	7	19	6	6	11	20
	20^3	2	2	13	34	2	2	13	34	5	5	22	35
	30^3	2	2	20	44	3	3	20	44	5	5	34	50
	40^3	3	3	27	58	3	3	27	61	5	5	46	70
	50^3	3	3	33	72	3	3	33	79	5	5	61	86
10^0	10^3	3	3	9	25	3	3	9	25	6	6	12	25
	20^3	3	3	18	44	3	3	19	44	5	5	35	48
	30^3	3	3	30	66	3	3	30	50	5	5	56	63
	40^3	3	3	41	73	3	3	41	73	5	5	66	82
	50^3	3	3	44	100	3	3	44	100	5	5	100	111
10^2	10^3	3	3	9	20	3	3	9	25	6	6	12	25
	20^3	3	3	20	44	3	3	20	44	6	6	37	48
	30^3	3	3	30	67	3	3	27	59	6	6	55	67
	40^3	3	3	40	73	3	3	40	73	6	6	76	86
	50^3	3	3	49	95	3	3	48	96	6	6	97	109

TABLE 4.1
BiCGStab iterations with an electric dipole source and uniform grids.

Non-uniform grids													
σ_c	# of	$\omega = 10^0$Hz				$\omega = 10^2$Hz				$\omega = 10^4$Hz			
(S/m)	cells	M_E	M_M	M_I	M_S	M_E	M_M	M_I	M_S	M_E	M_M	M_I	M_S
10^{-2}	30^3	1	3	18	47	3	3	18	49	5	5	34	52
	40^3	4	4	27	59	4	4	26	64	7	7	40	68
	50^3	2	2	28	76	2	2	28	71	4	4	48	84
10^0	30^3	3	3	26	65	3	3	26	62	5	5	55	76
	40^3	4	4	31	76	4	4	34	78	7	7	76	91
	50^3	2	2	43	101	2	2	43	102	4	4	98	139
10^2	30^3	3	3	25	65	3	3	25	64	6	6	53	76
	40^3	4	4	31	79	4	4	34	80	7	7	76	102
	50^3	2	2	43	105	2	2	43	102	5	5	100	132

TABLE 4.2
BiCGStab iterations with an electric dipole source and non-uniform grids.

All of the trials summarised in Tables 4.1–4.4 clearly show evidence of grid-independent rates of convergence of the BiCGStab method when preconditioned by M_E or M_M as opposed to M_I or M_S. In spite of the seemingly strong restrictions of the Fourier analysis of Section 3, the convergence behaviour of the exact block inversion M_E measures up to theoretical predictions. That is, the analysis succeeds in capturing the essential local behaviour of discrete operators for reasonable problems unhindered by the additional complications of non-uniform grids, of different boundary conditions, and, most significantly, of highly discontinuous conductivity models.

The results also show virtually identical performance in terms of iteration counts for the exact preconditioner M_E versus the single multigrid V(2,1)-cycle M_M. This observation suggests that solving the diagonal blocks exactly is unnecessary, at least within this frequency range. In particular, single V(2,1)-cycles work as effectively as

Uniform grids												
σ_c	# of	$\omega = 10^0$Hz				$\omega = 10^2$Hz				$\omega = 10^4$Hz			
(S/m)	cells	M_E	M_M	M_I	M_S	M_E	M_M	M_I	M_S	M_E	M_M	M_I	M_S
10^{-2}	10^3	1	4	6	13	4	4	6	13	4	4	6	13
	20^3	4	4	13	25	4	4	13	25	4	4	15	25
	30^3	4	4	19	32	4	4	19	32	4	4	21	32
	40^3	4	4	27	42	4	4	27	42	4	4	32	41
	50^3	4	4	32	51	4	4	32	53	4	4	36	53
10^0	10^3	4	4	6	13	4	4	6	13	4	4	6	13
	20^3	4	4	13	25	4	4	13	25	4	4	15	25
	30^3	4	4	19	32	4	4	19	32	4	4	21	32
	40^3	4	4	27	43	4	4	27	41	4	4	32	43
	50^3	4	4	32	51	4	4	32	51	4	4	37	48
10^2	10^3	5	5	7	13	5	5	7	13	5	5	7	13
	20^3	5	5	13	26	5	5	13	26	5	5	15	26
	30^3	4	4	19	32	4	4	19	32	4	4	22	32
	40^3	5	5	27	42	5	5	27	42	5	5	32	43
	50^3	5	5	31	52	5	5	31	50	5	5	37	56

TABLE 4.3
BiCGStab iterations with a magnetic source and uniform grids.

Non-uniform grids												
σ_c	# of	$\omega = 10^0$Hz				$\omega = 10^2$Hz				$\omega = 10^4$Hz			
(S/m)	cells	M_E	M_M	M_I	M_S	M_E	M_M	M_I	M_S	M_E	M_M	M_I	M_S
10^{-2}	30^3	1	3	23	41	3	3	23	42	3	3	25	42
	40^3	3	3	30	45	3	3	30	50	3	3	36	51
	50^3	2	2	37	61	2	2	37	60	2	2	47	62
10^0	30^3	3	3	23	42	3	3	23	41	3	3	26	41
	40^3	3	3	30	47	3	3	30	44	3	3	37	48
	50^3	3	3	37	60	3	3	37	65	3	3	47	65
10^2	30^3	3	3	21	41	3	3	21	41	4	4	27	48
	40^3	4	4	30	54	4	4	30	49	4	4	37	49
	50^3	3	3	37	57	3	3	37	57	4	4	47	59

TABLE 4.4
BiCGStab iterations with a magnetic source and non-uniform grids.

the preconditioner M_E with considerable savings in computational work.

Another interesting aspect of these results is that the iteration counts for all the preconditioners do not appear to depend strongly on ω or σ_c. Looking at Figure 3.1, we see that the spread of eigenvalues and the ℓ_2-condition number is quite flat until $\chi \simeq 10^1$. Once χ gets larger, however, the quadratic dependence of both quantities on χ becomes apparent and we can see the bound on the ℓ_2-condition number getting far worse. Since χ is at most $4\pi \times 10^{-1}$ in the trials so far, we do not observe the iterations changing much as σ_c and ω are varied within this range.

	# of	ω (Hz)					
	cells	10^1	10^2	10^3	10^4	10^5	10^6
M_M	30^3	3	3	3	6	12	98
	40^3	3	3	3	6	13	116
	50^3	3	3	3	6	12	128
M_I	30^3	30	27	31	55	166	642
	40^3	40	40	42	76	210	1180
	50^3	46	48	51	97	273	1551

TABLE 4.5
BiCGStab iterations for $\sigma_c = 10^2$ S/m for a range of frequencies.

To better observe the effect of increasing the parameter χ, we fix the underlying conductivity model with $\sigma_c = 10^2$ S/m and vary the frequency ω over a larger range. For these trials, we use an electric dipole source and count the number of iterations to convergence with problems discretised on uniform grids. We restrict our attention to the multigrid preconditioner M_M and the ILU preconditioner M_I. The results are summarised in Table 4.5.

The results of Table 4.5 demonstrate the degradation of both preconditioning strategies M_M and M_I with increasing frequency. As in the other trials, iteration counts for the ILU-preconditioned system grow as the grid is refined as opposed to the grid-independent iteration counts observed for the multigrid-preconditioned system. At the highest frequency $\omega = 10^6$ Hz, $\chi = 4\pi$. The performance of both preconditioners worsens significantly in increasing ω from 10^5 Hz to 10^6 Hz. This transition in convergence behaviour is consistent with the sharp rise we observe in $|\widetilde{\lambda}_{\max}|/|\widetilde{\lambda}_{\min}|$ and $\widetilde{\eta}_{\max}/\widetilde{\eta}_{\min}$ in Figure 3.1 near $\chi \simeq 10^1$. For general problems, the threshold frequency at which this transition occurs depends on the geometry of the problem (in particular, on the scales L, μ_0 and σ_0). However, the observations for higher frequencies agree well with the predictions of our Fourier analysis. This example is set over a short length scale but the same quantitative results apply in terms of iteration counts on larger domains.

The CPU-time required for each iteration[4] of the multigrid preconditioner is roughly 4 times more than that for the ILU preconditioner in case of a uniform grid, and roughly 8.5 times more in the case of the exponentially-widening grid (due to the additional cost of alternating-plane relaxations). Thus, using the ILU preconditioner M_I actually results in a faster algorithm than using the multigrid preconditioner M_M for coarse discretisations. But for fine discretisations (e.g., all cases recorded in Table 4.5) the multigrid preconditioner is to be significantly more efficient. Obviously, there is a crossover point beyond which the multigrid preconditioner is more efficient since it achieves convergence to a fixed tolerance within a constant number of iterations independent of the grid spacing h. In this example we see, moreover, that the crossover point occurs for grid sizes which are well within practical range. We feel that a more specific implementation of the multigrid cycle could improve the efficiency of the preconditioner further, and lead to an earlier crossover point.

The results presented here are based on a single geophysical model. We have also performed tests with other models as in [2, 16, 17] with qualitatively similar results.

Perhaps the greatest beauty of our multigrid approach as such is that the part which is hard to program is within a black box code already written by someone else. This is to be contrasted with all-out multigrid efforts such as [19] which achieve rapid convergence results but at a price in transparency and modularity (see also [5, 15]). A complete multigrid approach may perform better in cases where μ has large jump discontinuities, however, and we plan to address this in the future.

Acknowledgements. We thank Drs. J.D. Moulton and J. Dendy for very generous assistance in using BOXMG. We also thank Drs. E. Haber and D. Oldenburg for many helpful discussions and one of the referees for insightful comments.

REFERENCES

[4]The iteration times were compared by running trials with the preconditioners M_M and M_I on various machines. Precise computational work estimates for BOXMG can be found in [12, 11].

[1] R. E. Alcouffe, A. Brandt, J. E. Dendy, and J. W. Painter, *The multi–grid methods for the diffusion equation with strongly discontinuous coefficients*, SIAM J. Sci. Stat. Comput., 2 (1981), pp. 430–454.
[2] D. Aruliah, *Fast Solver for Time-Harmonic Maxwell's Equations in 3D*, PhD thesis, University of British Columbia, Dept. Computer Science, 2001.
[3] D. Aruliah, U. Ascher, E. Haber, and D. Oldenburg, *A method for the forward modelling of 3D electromagnetic quasi-static problems*, Math Models and Methods in Appl. Science, 11 (2001), pp. 1–21.
[4] R. Barrett, M. Berry, T. Chan, J. Demmel, , J. Donato, J. Dongarra, V. Eijkhout, R. Pozo, C. Romine, and H. V. der Vorst, *Templates for the Solution of Linear Systems: Building Blocks for Iterative Methods*, SIAM, Philadelphia, 1994.
[5] R. Beck, *Algebraic multigrid by component splitting for edge elements on simplicial triangulations*, tech. report, Konrad-Zuse-Zentrum, 1999.
[6] R. Beck, P. Deuflhard, R. Hiptmair, R. Hoppe, and B. Wohlmuth, *Adaptive multilevel methods for edge element discretizations of maxwell's equations*, Surveys Math. Indust., 8 (1999), pp. 271–312.
[7] A. Bossavit, *Computational electromagnetism. Variational formulation, complementarity, edge elements*, Academic Press, 1998.
[8] A. Brandt, *Multigrid techniques: 1984 Guide with applications to fluid Dynamics*, The Weizmann Institute of Science, Rehovot, Israel, 1984.
[9] T. Chan and H. Elman, *Fourier analysis of iterative methods for elliptic boundary value problems*, SIAM Review, 31 (1989), pp. 20–49.
[10] J. Demmel, *Applied Numerical Linear Algebra*, SIAM, 1997.
[11] J. Dendy, Jr., *Two multigrid methods for three-dimensional problems with discontinuous and anisotropic coefficients*, SIAM J. Sci. Stat. Comp., 8 (1987), pp. 673–685.
[12] J. E. Dendy, *Black box multigrid*, Journal of Computational Physics, 48 (1982), pp. 366–386.
[13] H. Elman, *Preconditioning for the steady-state Navier-Stokes equations with low viscosity*, SIAM J. Scient. Comput., 20 (1999), pp. 1299–1316.
[14] M. Everett and A. Schultz, *Geomagnetic induction in a heterogenous sphere: Azimuthally symmetric test computations and the response of an undulating 660-km discontinuity*, J. Geophys. Res., 101 (1996), pp. 2765–2783.
[15] J. Gopalakrishnan and J. Pasciak, *Overlapping Schwarz preconditioners for indefinite Maxwell equations*. Manuscript.
[16] E. Haber and U. Ascher, *Fast finite volume simulation of 3D electromagnetic problems with highly discontinuous coefficients*, SIAM J. Scient. Comput., 22 (2001), pp. 1943–1961.
[17] E. Haber, U. Ascher, D. Aruliah, and D. Oldenburg, *Fast simulation of 3D electromagnetic using potentials*, J. Comput. Phys., 163 (2000), pp. 150–171.
[18] W. Hackbusch, *Multi-Grid methods and Applications*, Springer-Verlag, 1985.
[19] R. Hiptmair, *Multigrid method for Maxwell's equations*, SIAM J. Numer. Anal, 36 (1998), pp. 204–225.
[20] J. Jin, *The Finite Element Method in Electromagnetics*, John Wiley and Sons, 1993.
[21] C. Matiussi, *An analysis of finite volume, finite element, and finite difference methods using some concepts from algebraic topology*, J. Comput. Phys., (1997), pp. 289–309.
[22] J. D. Moulton, *Numerical implementation of nodal methods*, PhD thesis, Institute of Applied Mathematics, University of British Columbia, 1996.
[23] G. Newman and D. Alumbaugh, *Frequency-domain modelling of airborne electromagnetic responses using staggered finite differences*, Geophys. Prospecting, 43 (1995), pp. 1021–1042.
[24] I. Perugia, V. Simoncini, and M. Arioli, *Linear algebra methods in a mixed approximation of magnetostatic problems*, SIAM J. Scient. Comput., 21 (1999), pp. 1085–1101.
[25] R. Richtmyer and K. Morton, *Difference Methods for Initial-Value Problems*, Wiley, 1967.
[26] Y. Saad, *Iterartive Methods for Sparse Linear Systems*, PWS Publishing Company, 1996.
[27] S. Selberherr, *Analysis and Simulation of Semiconductor Devices*, Wien: Springer-Verlag, 1984.
[28] A. Taflove, *Computational Electrodynamics: the Finite-Difference Time-Domain Method*, Artech House Publishers, 1995.
[29] C. Weaver, *Mathematical Methods for Geo-Electromagnetic Induction*, John Wiley & Sons Inc, Philadelphia, 1994.
[30] P. Wesseling, *An Introduction to Multigrid Methods*, John Wiley & Sons, Chichester, 1992.
[31] D. Zwillinger, ed., *Standard Mathematical Tables and Formulae*, CRC Press, 1996.